Electron- and photon-stimulated modification of GaAs(110), Si(100), and Si(111)

B. Y. Han, Koji Nakayama, and J. H. Weaver
Department of Materials Science and Chemical Engineering, University of Minnesota, Minneapolis, Minnesota 55455
(Received 15 June 99)

Scanning tunneling microscopy results show that irradiation with electrons of primary energies of 90–2000 eV created single-layer deep vacancies on GaAs(110), Si(100), and Si(111). The removal yield was linear with dose during the initial stages of surface modification, but it increased as the surface damage increased. The cross section varied with primary electron energy, increasing from $4.4\times10^{-20}\,\mathrm{cm}^2$ at 100 eV to $1.8\times10^{-19}\,\mathrm{cm}^2$ at 2000 eV for GaAs(110) and from $1\times10^{-20}\,\mathrm{cm}^2$ at 90 eV to $5\times10^{-20}\,\mathrm{cm}^2$ at 2000 eV for Si(111)-7×7. The mechanisms responsible for atom displacement and desorption involve excitations in the surface region achieved by the cascade of inelastically scattered electrons. Processes involving long-lived localized states facilitate the coupling to the nuclear motion needed for atom displacement, with details that reflect surface reconstructions, surface states, and defect levels. Once surface defects have been created by electron irradiation of GaAs(110), they can be expanded by irradiation with photons of energy 2.3 eV. Photon irradiation involves site-selective desorption, and this allows patterning and atomic layer removal. [S0163-1829(99)07043-5]

I. INTRODUCTION

Electrons play an essential role in many areas of surface analysis and materials characterization.[1] For example, Auger electron spectroscopy (AES) and low energy electron diffraction (LEED) are used routinely to study the compositional and crystallographic properties of surfaces, using electrons with energies of 20–5000 eV. Electron microscopies using higher energy electrons offer opportunities to investigate bulk structural properties. Damage can be produced by momentum transfer from electrons to surface atoms, as is particularly well recognized for high energy beams with intensities of $10^2-10^3\,\mathrm{A\,cm}^{-2}$ and kinetic energies of 141–200 keV.[2] At lower intensity and kinetic energy, electrons are well known to stimulate the desorption of adsorbates from surfaces,[3] as well as cause desorption of intrinsic atoms from ionic solids.[4,5] They have not, however, been implicated in the modification of clean semiconductor or metal surfaces.

In this paper, we examine GaAs(110), Si(100), and Si(111) surfaces exposed at room temperature to beams of electrons having primary energies of $90\,\mathrm{eV}\leqslant E_p\leqslant 2000\,\mathrm{eV}$ and current densities of 0.1–10 mA cm^{-2}. Using scanning tunneling microscopy (STM), we show that small vacancy complexes are created randomly on these surfaces. These modifications occur as a consequence of electronic excitations, and they are manifest by the desorption of intrinsic atoms or their transfer onto the surrounding terrace.[6] Moreover, the efficiency of this process increases with electron energy. Though not thought to be important for semiconductor surfaces, the underlying phenomena are analogous to those encountered in adsorbate-surface systems, namely desorption induced by electronic excitations (DIET).[3–5]

Figure 1 shows a generic potential energy curve where the lower line represents the system in its ground state, with equilibrium at the minimum, and the upper state corresponds to an unstable configuration where an increased nuclear separation would lower the total energy. These unstable configurations can be reached through the inelastic scattering of primary electrons and their production of a cascade of lower energy states distributed in the surface region, as depicted at the bottom of Fig. 1. With incident energies of 90–2000 eV, electrons and holes can be produced throughout the conduction and valence bands, and their number increases with primary energy. If localized states at the surface are involved, then energy can be transferred from the electronic to the

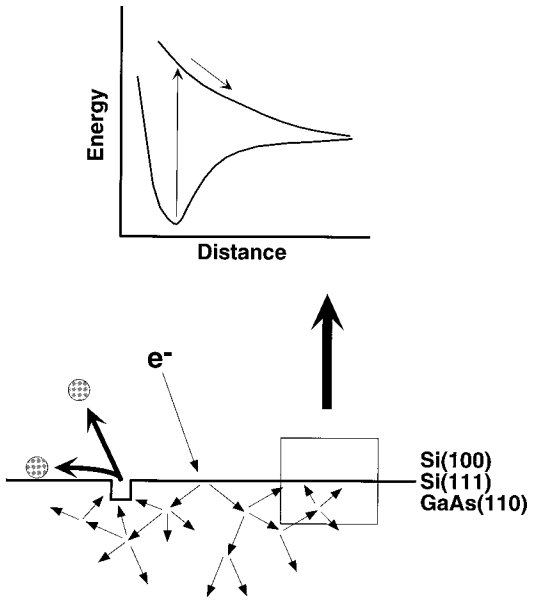

FIG. 1. Depiction of electron- and photon-stimulated surface modification. The top panel shows potential energy curves representing the ground state and an unstable repulsive state reached by electronic excitation or photon absorption. Relaxation via nuclear motion results in bond breaking and atom transfer onto the surface or into the gas phase can occur. The lower panel depicts multiple inelastic scattering for electrons incident on the surface. The cascade results in occupation of electron and hole states over a wide energy range, and these carriers activate the transition in the top panel.

nuclear system and bonds can be destabilized.[3] Candidates for localized states include surface states, surface resonances, and defect levels associated with vacancies and steps.

The second focus of this paper also involves surface modifications due to electronic processes, but the relevant electronic states are those achieved following photon adsorption. Starting from GaAs(110) surfaces with vacancies introduced by electron bombardment, we show that the top layer can be removed by pulsed-laser irradiation with 2.3-eV pulses at power levels below the photothermal threshold. In this case, there is selective desorption of atoms from boundaries of existing pits and the pits expand in the top layer. This again involves localized defect or pit levels and reduced bonding at these sites. The importance of these states is demonstrated by equivalent irradiation of defect-free surfaces since no damage was introduced. Together, these results suggest ways to modify and pattern surfaces without introducing extrinsic elements.

II. EXPERIMENTAL TECHNIQUES

The experiments were performed in ultrahigh vacuum chambers with base pressures better than 1×10^{-10} Torr. For GaAs, pristine (110) surfaces were obtained by cleaving posts that were Zn-doped at $1\times10^{18}\,\mathrm{cm}^{-3}$. These posts and their supports were thoroughly degassed before cleaving to minimize subsequent contamination induced by irradiation of their sides. The cleaved surfaces had defect levels below ~0.3%, mostly in the form of point defects or adatoms. For Si(100) and Si(111), we used *p*-type wafers that were *B*-doped at 0.01 Ω cm and 0.005–0.013 Ω cm, respectively. We also irradiated Si(100)-2×1 samples that were *B*-doped at 3×10^{17} and $9\times10^{18}\,\mathrm{cm}^{-3}$ and *P*-doped at $5\times10^{18}\,\mathrm{cm}^{-3}$, but there was no significant dependence on dopant type or concentration. Si(100)-2×1 and Si(111)-7×7 surfaces were prepared by thermal treatment.[7,8]

Electron guns from a Varian LEED system and a Perkin-Elmer AES system were used to obtain beams of $90\leqslant E_p\leqslant400$ eV and $400\leqslant E_p\leqslant2000$ eV for normal incidence irradiation. The beam profiles at the sample position were approximately Gaussian with a $1/e$ diameter of ~1.5 mm, as measured with a Faraday cup having a 0.5-mm diameter aperture. STM images obtained within about 0.5 mm of the center of the electron-irradiated area revealed approximately homogeneous defect distributions. The current densities were 0.1–10 mA cm^{-2}, corresponding to fluxes of 6.3×10^{14}–$6.3\times10^{16}\,\mathrm{cm}^{-2}\,\mathrm{s}^{-1}$. The guns were thoroughly degassed before each run so that the pressures during irradiation did not exceed 4×10^{-10} Torr. To verify that the hot filaments were not causing enhanced adsorption of residual gases, we placed freshly cleaved or cleaned samples at the usual irradiation position for 20 min while the filaments were operating but with no bias (no emission). STM images showed no increase in the defect density.

Auger electron spectroscopy was used to check for surface carbon and oxygen buildup on Si(100)-2×1, the most reactive of the three surfaces studied. The carbon concentration was below 1% after 300-s electron irradiation at 2000 eV and 10 mA cm^{-2}. The accumulation rate was 3.2×10^{-5} ML s^{-1} for times less than 2000 s. The oxygen concentration was even smaller.

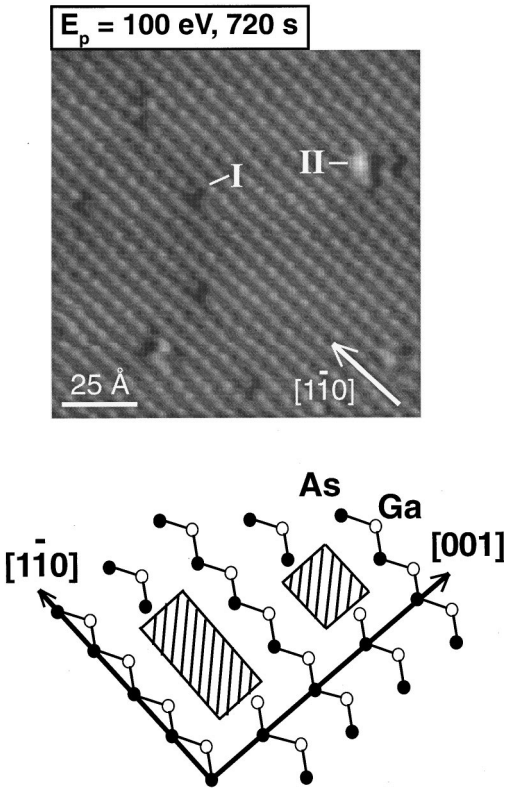

FIG. 2. STM image of GaAs(110) following 720-s irradiation with 100-eV electrons at a current density of 0.1 mA cm^{-2}. Small pits such as ''I'' appear as dark depressions in the $[1\bar{1}0]$ rows. Most of them correspond to a single Ga-As pair vacancy, as depicted. Feature ''II'' probably reflects an As adatom.

A frequency-doubled Nd:YAG laser was used to irradiate GaAs(110) with 2.3 eV photons. The beam was coupled to the measurement chamber through a quartz window. The pulse energy intensity was low, 35 mJ cm^{-2}, to avoid damage due to ablation.[9] The pulse duration was 6 ns.

Scanning tunneling microscope images were obtained at room temperature for the starting surfaces and after electron or photon exposure. Most were constant-current, occupied-state images which, for GaAs, revealed the As sublattice. The tip voltages were 1.8–3.2 V and tunneling currents were 0.1–0.2 nA. Dual bias images were taken occasionally.

III. RESULTS

A. Electron irradiation of GaAs(110)

Figure 2 shows a STM micrograph of GaAs(110) obtained after irradiation with 100-eV electrons. The flux was $6.3\times10^{14}\,\mathrm{cm}^{-2}\,\mathrm{s}^{-1}$ and the duration was 720 s, giving a dose of $4.5\times10^{17}\,\mathrm{cm}^{-2}$. Irradiation produced small, single-layer-deep pits that appeared as dark depressions in the $[1\bar{1}0]$ rows. Most were confined to one row, such as that labeled I. The ends of the pits had well-defined appearances that indicated whether they were terminated by Ga or As, as confirmed by dual-bias imaging.[10] The pit density in images like Fig. 2 was $5\times10^{12}\,\mathrm{cm}^{-2}$, and they accounted for about 2% of the top layer (0.02 ML). The removal yield was 3.9×10^{-5} atom/electron. Dividing the yield by the surface atom density gives a cross section of $4.4\times10^{-20}\,\mathrm{cm}^2$.

Analysis of dozens of images showed that about 70% of the pits correspond to the removal of one Ga-As pair, as depicted in the schematic of Fig. 2. Also depicted is a pit derived from two pairs. There were approximately equal numbers of Ga and As atoms at pit boundaries for both low dose (Fig. 2) and higher doses, suggesting no preferential removal. The terminating atoms for pits along $[1\bar{1}0]$ are nominally twofold coordinated, although rebonding with second layer atoms of the same species would be possible. Such atoms are less well bound than terrace atoms, and there are different energy levels associated with them.

The bright feature labeled II in Fig. 2 is located between rows of As atoms. It appears to be bonded to a surface Ga atom. Similar features were found on GaAs(110) after sputtering with inert ions[11] and after etching with Br.[10] They have been attributed to As adatoms, and they can be eliminated by annealing. Annealing also results in structural changes due to thermally activated vacancy diffusion, as discussed by Pechman *et al.*[12] in the context of vacancy coalescence on ion-sputtered GaAs(110).

The effects of increasing the electron dose can be seen in Fig. 3 for 400-eV electrons, though equivalent trends were observed with electrons of higher and lower energies. In Fig. 3(a), most of the pits were derived from a missing Ga-As pair, the pit density was $5\times10^{12}\,\mathrm{cm}^{-2}$, and the pit area was 0.02 ML. The flux was the same as in Fig. 2, but the exposure time was half as much so the yield was approximately twice that for 100-eV electrons. The pit density and area increased linearly with time to 900 s, Fig. 3(b), indicating that removal events occurred randomly at low dose. By 1440 s, however, there were pits that extended over several unit cells, both along and across the $[1\bar{1}0]$ rows, Fig. 3(c). At this point, the pits represented an appreciable portion of the surface, and pit growth became more important. Significantly, there was no preferred growth direction for electron irradiation. The dependence of damage on dose is summarized in Fig. 4(a) where the dashed curves represent linear extrapolations of the low-dose regime.

The dependence of removal yield on primary electron energy for GaAs(110) is summarized in Fig. 5 in the low dose regime. Increasing the energy from 100 to 400 eV doubled the yield. Increasing it to 2000 eV again doubled it, to 1.6×10^{-4} atom/electron. The tendency of increased yield with kinetic energy might seem surprising at first, since the electron inelastic mean free path has a minimum at 50–100 eV and higher energy electrons have a smaller probability of inelastic scattering in the surface layer. However, these more energetic electrons produce a larger number of cascade scattering events, thus generating more carriers that can participate in surface excitations and modifications. Our experimental results for GaAs and for Si show that this cascade process is more important than the mean free path of the primary electron.

The ratio of the removal yields from GaAs(110) terrace sites and pit boundaries can be estimated from the deviation of the total removal yield from the linear dependence of Fig. 4(a). While approximate, it highlights the role of defects in enhancing electron-stimulated damage. From the schematic in Fig. 2, a single Ga-As vacancy exposes the four neighboring unit cells, a double vacancy exposes six, and so on. For 0.05-ML removal, Fig. 3(b), about 60% of the pits are single

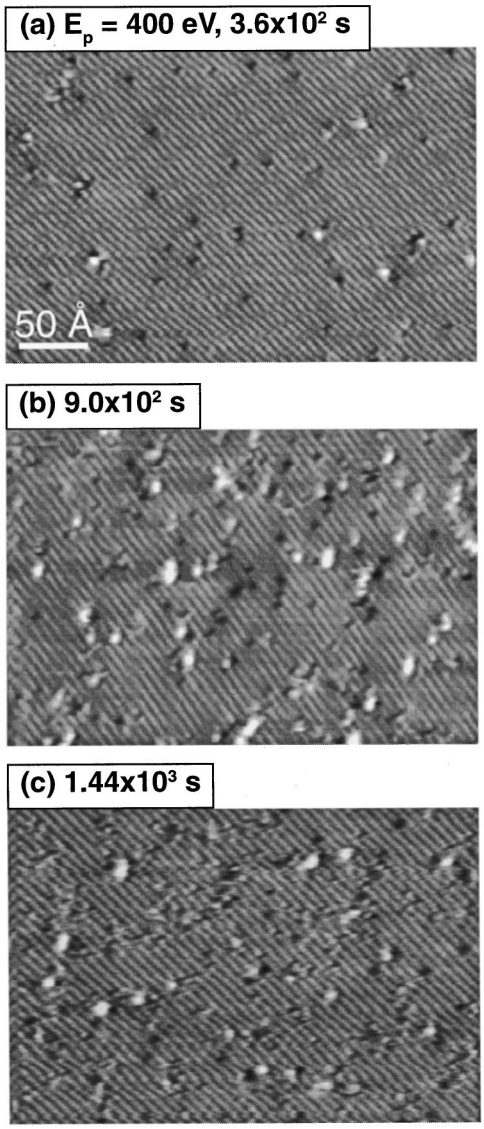

FIG. 3. STM images obtained after irradiation with 400 eV electrons at a current density of 0.1 mA cm^{-2}, as in Fig. 2. The vacancy areas amount to 0.02, 0.05, and 0.09 ML in (a)–(c). Larger pits are more frequent at higher dose, with (c) reflecting desorption from edges of existing pits.

Ga-As vacancies. The overall average number of unit cells around a pit is ~5, and the total number of unit cells bordering them corresponds to approximately $5\times(1.2\times10^{13})/(4.42\times10^{14})=0.14$ ML. Terrace sites not involved with pits or pit boundaries amount to 0.81 ML. From Fig. 4, linear extrapolation leads to a vacancy area of 0.08 ML after 1440 s, compared to 0.09 ML from experiment. If η is the ratio of removal yield from boundaries relative to terrace sites, then $0.14\eta+0.81\approx(0.09-0.05)/(0.08-0.05)$, and the desorption probability from a pit boundary is roughly ~4 times that from a terrace site. This treats all pit boundaries sites as equivalent since no significant growth anisotropy was found.

Figure 6 shows that extended electron irradiation eventually resulted in multilayer erosion (2000-eV beam energy, current density 0.3 mA cm^{-2}, and dose $1.7\times10^{18}\,\mathrm{cm}^{-2}$). About 40% of the top layer had been removed, and the residual areas were irregular and fragmented. The small bright features on the top layer are attributed to As adatoms, as in

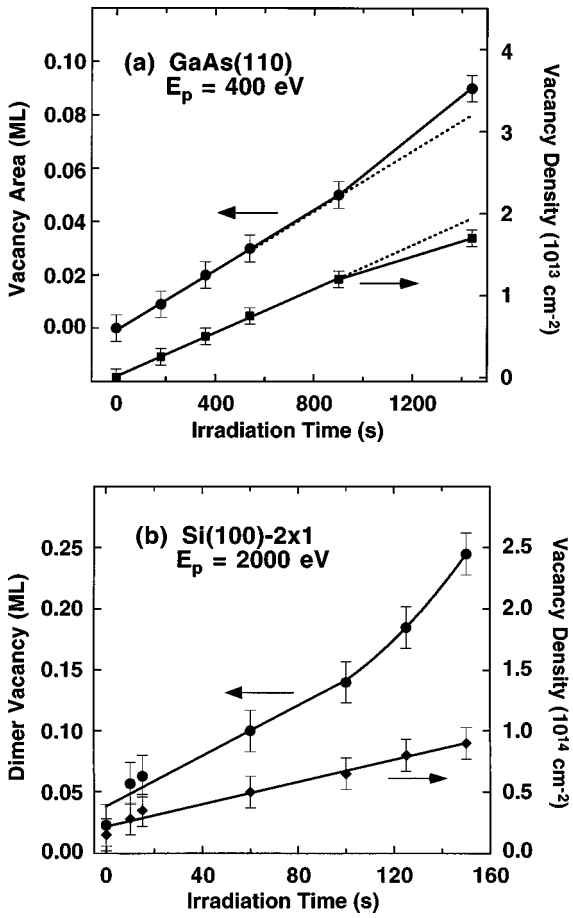

FIG. 4. (a) Vacancy area and vacancy complex density vs irradiation time for GaAs(110) for 400-eV electrons (current density 0.1 mA cm^{-2}, flux 6.3×10^{14} cm^{-2} s^{-1}). The areas and densities increase linearly until ~900 s and vacancy creation is random. Thereafter, the defect density increases as removal from existing pits plays a greater role. Similar trends were observed for 100 and 2000 eV electrons with current densities of 0.03–1 mA cm^{-2}. (b) Dimer vacancy area and vacancy complex density for Si(100)-2×1 for 2000-eV electrons (flux 6.4×10^{16} cm^{-2} s^{-1} corresponding to ~100 incident electrons per second for each surface atom). Vacancies are created randomly until ~100 s but the accumulation of damage enhances further removal.

Fig. 1, while the large ones are probably Ga clusters. Pitting of the second layer is evident from dark patches inside large single-layer pits. Second layer defects were usually located at the edges of first layer pits, suggesting that these edges have electronic states that are particularly effective in localizing charge. For these surfaces, regrowth structures were unlikely because of the limited mobility of adatoms at room temperature. If these samples were heated, the residual As would desorb, vacancies would be accommodated at steps, and the step irregularity would be reduced. Such recovery would be sluggish because of the high defect density, as discussed below for Si(100)-2×1.

B. Electron irradiation of Si(100)-2×1

Figure 7 summarizes the effects of electron irradiation of Si(100)-2×1. Images like Fig. 7(a) of the clean surface reveal rows made up of dimers that appear as oval structures,

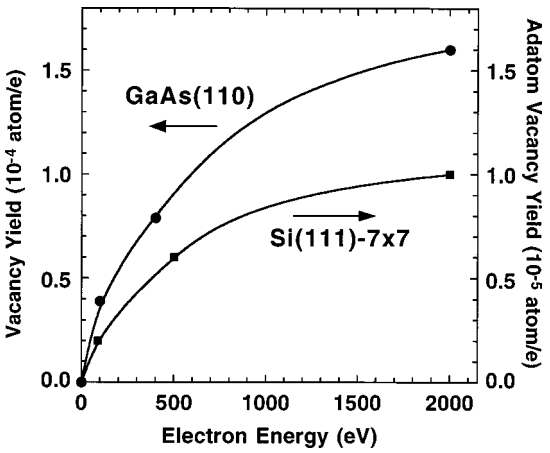

FIG. 5. Vacancy yield as a function of incident electron energy for atoms of the adatom layer of Si(111)-7×7 and for GaAs(110). The dependence on kinetic energy is correlated with the number of cascade scattering events and the number of carriers that can participate in electronic transitions or capture events, as shown in Fig. 1.

due to their dynamic buckling.[7] Steps and defects quench the buckling, and the now-asymmetric dimers appear as bright protrusions on alternate sides of successive dimers along a row, as labeled *B*. For our surfaces, dimer vacancies (DV) and *c*-type defects (CD) (Refs. 13, 14) were about equal in number. Their total concentration was ~4%, as is typical for surfaces prepared by heating.[7,8]

Figure 7(b) shows that irradiation greatly increased the concentration of single DV's and *c*-type defects (2000 eV at 10 mA cm^{-2} for 150 s for a dose of 9.6×10^{18} electrons cm^{-2}). There were also dimer vacancy complexes (DV_C) that extended along and across the dimer rows. Inspection of the step profiles revealed increased roughness, as in Fig. 7(b). While single adatoms could not be imaged, the bright spots labeled A_1, A_2, and A_3 correspond to ad-dimers formed from atoms displaced onto the terrace. Their geometries agree with those deduced for dimers trapped in non-

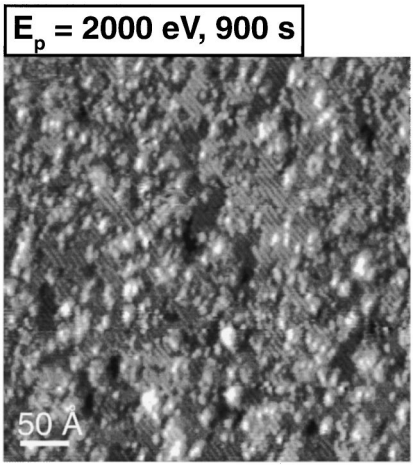

FIG. 6. Multilayer erosion occurs after extended irradiation of GaAs(110) with 2000 electrons (0.3 mA cm^{-2} for 900 s giving a dose of 1.7×10^{18} cm^{-2}). About 40% of the original top layer was removed and residual areas were highly fragmented. Dark patches indicate damage to the exposed second layer.

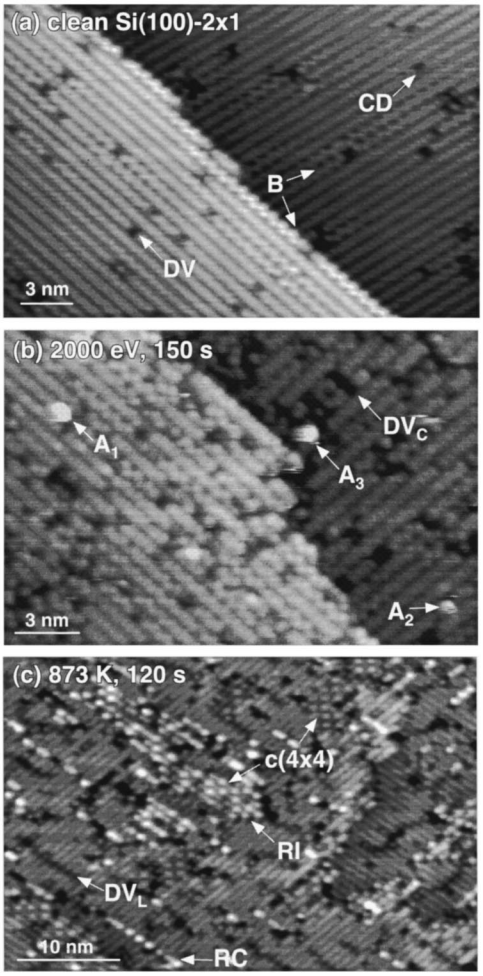

FIG. 7. (a) Filled state image of clean Si(100)-2×1 showing dimer vacancies (DV), *c*-type defects (CD), and a row of asymmetric buckled dimers (B) at a step (sample: 2.0 V, 0.2 nA). (b) Image showing dimer vacancy complexes (DV_C) produced by irradiation with 2000-eV electrons for 150 s (flux 10 mA cm^{-2}, dose 9.6 $\times 10^{18}$ cm^{-2}). Ad-dimers are labeled A_1 if their axis is parallel to the dimer row, A_2 if they lie perpendicular to the row, and A_3 if they reside between rows. (c) Annealing surfaces like that in (b) produces dimer vacancy lines (DV_L), regrowth chains (RC), and regrowth islands (RI). $c(4\times4)$ patches appear near steps and in regrowth areas.

ideal configurations after Si deposition on Si(100)-2×1.[15–18] They were unstable with respect to tip-induced motion under typical imaging conditions (sample bias −2 V, tunneling current 0.2 nA).[15]

As summarized in Fig. 4(b), the dimer density and vacancy area increased approximately linearly with dose until ~ 100 s, rising from 0.02 ML for the clean surface. While the density of DV's more than quadrupled, from 0.14 to 0.65×10^{14} cm^{-2}, the average size of a vacancy complex increased only ~50%. For Si(100), the (low-dose) vacancy creation cross section was 1.2×10^{-20} cm^2, smaller by an order of magnitude compared to GaAs(110), and vacancy production was largely random. After ~ 100 s irradiation, the vacancy concentration increased nonlinearly as defects influenced the probability of material removal adjacent to them. The pit growth apparent in Fig. 7(b) reflects the tendency of defects to localize electronic excitations and to increase inelastic scattering events. Pit growth may also reflect the reduced energy barrier for atom displacement at a pit boundary compared to a terrace site.

For Si(100)-2×1, the event that creates a single atom vacancy is followed by the escape onto the terrace of the now-unpaired atom of the original dimer. The initial vacancy can be created by either single atom desorption or displacement onto the terrace. The features imaged as dimers or aggregates in Fig. 7(b) reflect the sum of the displaced atoms, less any single atoms because the latter cannot be imaged. Since the terrace features account for only ~20% of the DV's (total cross section for vacancy creation 1.2×10^{-20} cm^2), we conclude that electron-stimulated desorption is significant. Note that the annihilation of a dimer vacancy would require capture of two diffusing atoms, and this is unlikely at 300 K. Accordingly, damage accumulation is particularly profound for Si(100).

Heating surfaces like that of Fig. 7(b) to 873 K for 120 s produced regrowth chains and islands on the terraces, labeled RC and RI in Fig. 7(c).[19,20] Moreover, small domains with $c(4\times4)$ symmetry appeared at steps and in regrowth islands, as for epitaxial growth of Si on Si(100).[21] Thermally activated diffusion of individual dimer vacancies allowed them to order into lines that were perpendicular to the dimer rows, DV_L. Recovery of a surface that was this severely damaged was sluggish because defects reduced terrace diffusion and influenced the (local) energetics associated with islands or steps. Annealing at 500 K for 30 min enhanced healing for lightly damaged surfaces but produced no significant change in morphology for surfaces like Fig. 7(b). Slow recovery was also observed when surfaces damaged by ion bombardment were annealed at 873–1123 K.[22]

C. Electron irradiation of Si(111)-7×7

Figure 8 summarizes results for electron modification of Si(111)-7×7. For the clean surface, the bright features within a 7×7 unit cell represent the corner adatoms adjacent to (dark) corner holes and center adatoms away from those holes. Irradiation produced vacancies in the adatom layer, as shown in Figs. 8(b)–8(d) for a fluence 2×10^{18} cm^{-2}.

Irradiation with 90-, 500-, and 2000-eV electrons increased the concentration of vacancies in the adatom layer from 4% (clean surface) to 6, 10, and 14%, respectively, as shown in Fig. 8. The ratio of vacancies at center sites relative to corner sites increased from 1:1 to 1:1.2 after irradiation for all energies, and single adatom vacancies appeared 1.3 times more frequently in the faulted half of the unit cell. The mean distance between vacancies decreased from ~28 Å for the clean surface to 20 Å after irradiation with 90-eV electrons. After 2000-eV irradiation, ~50% of the vacancies were present in nearest-neighbor configurations, and complexes derived from up to 7 adatom vacancies were evident. The number of such complexes increased with dose as vacancies influenced removal of nearby adatoms.

Figure 5 shows how the yield for adatom vacancy generation depends on the primary electron energy. The steady increase with primary energy is significant because it indicates that Si core level excitations followed by Auger decay were not important in surface atom desorption, in contrast to what has been demonstrated for ionic materials.[5] (The cross sec-

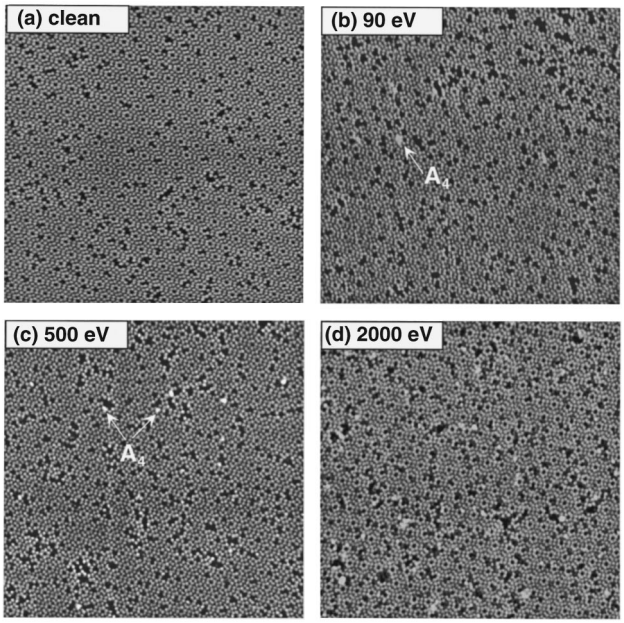

FIG. 8. Images for Si(111)-7×7 before (a) and after irradiation by electrons with primary energies of (b) 90 eV, (c) 500 eV, and (d) 2000 eV for a common total dose of $2\times10^{18}\,\mathrm{cm}^{-2}$. Vacancies in the adatom layer appear as dark features. They are largely due to Si desorption, though features like A_4 represent Si atoms trapped at rest-atom dangling bonds. Desorption is random when the vacancy concentration is low. ($500\times500\,\text{Å}^2$; sample bias 1.7 V, tunneling current 0.4 nA.)

tions for such core level excitation would increase above the Si $2p$ and $2s$ excitation thresholds of ~100 and 150 eV but would then decrease as $1/E_p$.) As for GaAs(110), we attribute the increase in the yield to the larger number of low energy carriers produced by cascade scattering and their localization at surface resonances or defect levels.

Features like A_4 in Fig. 8 represent Si released from adatom sites and trapped at dangling bond sites of rest atoms. These extra terrace atoms were outnumbered by the vacancies by a factor of ~30 after irradiation with 90- and 500-eV electrons. Neglecting them, the cross section for Si desorption from Si(111)-7×7 follows directly from Fig. 5, ranging from $1\times10^{-20}\,\mathrm{cm}^2$ for 90-eV electrons to $5\times10^{-20}\,\mathrm{cm}^2$ for 2000-eV electrons. (Accommodation of the missing atoms at steps was negligible because the terraces were ~1500-Å wide.) These values fall within the range reported for electron-stimulated desorption of adsorbates on surfaces.[4,5] While the vacancy yield is ~16 times higher for GaAs(110) than for Si(111)-7×7 at 2000 eV, the difference in cross section is only ~3.5 when account is taken for the planar density of terrace and adatom layer atoms.

The cross section for desorption is a measure of long-term surface modification, but it underestimates defect formation for Si(111)-7×7 because a vacancy in the adatom layer can be annihilated by a single diffusing atom. This effect was recently studied by Stipe *et al.*,[23] using STM to displace an adatom and to follow its return. They showed that adatom layer vacancies were short lived above 175 K. Our results therefore underestimate the importance of electron beam irradiation and the complete structural response of the 7×7 surface should be probed at low temperature.

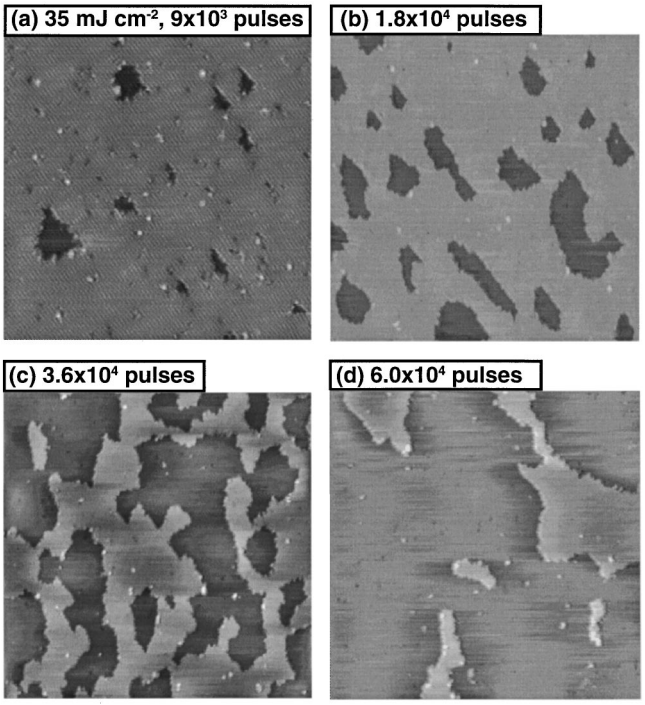

FIG. 9. (a)–(d) STM images showing the effect of photon-stimulated desorption from an electron-irradiated surface of GaAs(110) equivalent to Fig. 2(a) [hv=2.3 eV, ~35 $\mathrm{mJ\,cm}^{-2}$, pulse duration ~6 ns.] Desorption occurs from defects and pit boundaries with preferential pit expansion along $[1\bar{1}0]$. The removal yield is related to the total length of pit edges and the details of defect levels. Extended photon irradiation results in removal of the top layer. [(a) $500\times500\,\text{Å}^2$; (b)–(d) $750\times750\,\text{Å}^2$].

D. Site selective photon-stimulated desorption on GaAs(110)

The above has emphasized defect creation caused by electron irradiation. In the following, we consider the growth of those defects due to photon irradiation. The underlying processes initiating the displacement of an atom from its equilibrium site are the same, namely the capture of a carrier in a surface state or a defect or pit level. A key difference is that energetic electron irradiation accesses a wide range of states, while only those within 0.9 eV of the band edges can participate after 2.3-eV photon absorption. This difference can be used to advantage, as shown below.

In these photodesorption studies, we first cleaved GaAs(110) to produce pristine surfaces and then exposed them to electrons to introduce point defects. Figure 9 summarizes results for a surface having an initial defect density of $4.5\times10^{12}\,\mathrm{cm}^{-2}$ and a defect area of 0.02 ML. Irradiation with 9×10^3 pulses increased the pit area to 0.10 ML, see Fig. 9(a). Equivalent irradiation of pristine surfaces showed that no pits formed and we conclude that removal was limited to sites around existing pits.[9,24] The yield was then 8×10^{-8} atom/photon (photon number density $9.4\times10^{16}\,\mathrm{cm}^{-2}$ per pulse). The robustness of terrace sites reflects the delocalized nature of excitations accessible with 2.3-eV photons[25] and the absence of localized gap states.[26] In contrast, the significant yield for pit boundary atoms reflects the localized nature of defect levels and the fact that these sites are natural carrier recombination sites.

Between Figs. 9(a) and 9(b), the pits expanded from 0.10 to 0.22 ML, giving a yield of 1.3×10^{-7} atom/photon. This is larger than for the first increment of pulses because of the higher linear density of pit edges.[9] Moreover, the rate of expansion increases for the larger pits. The elongated pits in Fig. 9(b) indicate that removal is favored along $[1\bar{1}0]$. Steps develop along $\langle 11n\rangle$, $[1\bar{1}0]$, and [001] as pits grow, reflecting the existence of defect levels and preferential removal of kink atoms due to their weaker bonding. The shapes of the large pits indicate coalescence. Continued irradiation reduced the top layer to 0.49 and 0.24 ML, Figs. 9(c) and 9(d), with a declining yield as the total edge length decreases.

Continued irradiation to 1.8×10^{5} laser pulses removed more than 95% of the top layer with the remnants evident as scattered islands made up of several to several tens of atoms. At this stage, there was also limited erosion of the second layer, 4–5%, probably due to subsurface defects created during the initial electron bombardment. Again, equivalent laser irradiation of pristine cleaved GaAs(110) showed minimal pitting events (below 0.3%).

IV. DISCUSSION

From the above, it is clear that electrons with energies of 90–2000 eV can produce surface defects on pristine Si(100), Si(111), and GaAs(110). Moreover, 2.3-eV photons are effective at removing atoms from defect sites of GaAs(110). Insight can be gained by comparing with results in the literature regarding electron and photon irradiation.

Low energy electrons are used in STM imaging, and the surfaces of Si and GaAs have been exhaustively studied. We and others have found no evidence for defect creation for pristine Si(100) or GaAs(110) under typical tunneling conditions of $\pm$(1.8–3.2) V and 0.1–0.2 nA. Typical current densities in the tunneling junction, through an area of atomic or at most nanometer dimensions, are orders of magnitude higher than in the present electron-irradiation experiments. Hence, direct carrier transfer to populate electron or hole states in this energy window does not cause atom displacement for Si(100)-2×1 or GaAs(110). Similarly, the absence of surface modification following laser irradiation of pristine Si(100)-2×1[27] or GaAs(110) confirms the inaccessibility of unstable configurations of the sort depicted in Fig. 1.

The Si(111)-7×7 surface responds differently to both low energy electrons and photons. Stipe *et al.*[23] demonstrated that the injection of carriers from an STM tip biased at $-$(3–10) V causes atom displacement from the adatom layer. They attributed the effect to electron occupation of a surface resonance associated with *s*-like Si adatom orbitals. Using low power laser irradiation, Kanasaki *et al.*[28] measured the desorption efficiency for Si atoms from Si(111)-7×7 as a function of photon energy. They reported a strong enhancement centered at about 2 eV, and they attributed the enhancement to dipole transitions involving surface states and site localization.

Localized energy levels have also been probed for Si(111) with adsorbed oxygen. In this case, Martel *et al.*[29] linked desorption to electron capture in antibonding resonances initiated by ~7 eV electrons from the tip. Shen *et al.*[30] tied the desorption of H from H-saturated Si(100)-2×1 to transitions from σ(Si-H) bonding levels to σ^*(Si-H) antibonding levels caused by ~6-eV electrons from an STM tip.

Whereas defect creation has not been observed following low energy electron or photon irradiation of pristine Si(100) and GaAs(110), our results show that they can be created with 90–2000 eV electrons. By analogy to low energy processes for Si(111) and for adsorbates, we attribute atom displacement to localized levels that have not been accessible previously. In particular, cascade scattering accesses states throughout the valence and conduction bands and localization at a surface site accounts for displacement of the sort depicted in Fig. 1. This is supported by the fact that vacancy creation occurred randomly on ideal terraces and increased with primary energy as the number of hot carriers that can reach the surface increased.

Our results for photon-stimulated desorption from GaAs(110) also point to the importance of localized levels since desorption does not occur from defect-free terraces. The importance of defect sites on GaP(110) and GaAs(110) was first demonstrated by Itoh and coworkers when they investigated laser-induced desorption.[25] They recognized the connection to electronic excitations, based on dependencies on energy and intensity. Starting with surfaces that were sputter-annealed, they observed the onset of emission and the subsequent reduction of emission with time. From this, they inferred different sites for desorption. Our recent STM studies of GaAs(110)[9] provided insights into the relevant sites by showing that pits created by Br etching could be expanded using 2.3-eV photons. The role of defects was also demonstrated for Si(100)-2×1 with a significant vacancy concentration.[31] In that case, laser-induced surface dimer removal was observed and, since heating was insufficient to induce thermal desorption, material removal was attributed to electronic transitions involving defect levels.

There are important implications that follow from these observations. For metals, activation barriers for vacancy creation are much lower, but electronic states are more delocalized. Although the cross section for desorption from metal surfaces is low, surface vacancies may be created by electron irradiation or by secondary electrons produced after high energy photon absorption. Indeed, Ernst *et al.*[32] recently demonstrated vacancy creation for Cu(111) and (100) by tuning the photon energy of a laser to excite electrons from localized *d*-band states. For semiconductors, surface vacancies may be created by secondary electrons produced after high energy photon absorption. In all cases, defects introduced by the beam probe would alter the local reactivity.

A combination of random defect creation with electrons and site-selective desorption with photons makes it possible to achieve atomic layer removal. Compared to chemical etching or ion sputtering, this procedure has the advantage that it does not introduce extrinsic elements and it causes minimal damage to the subsurface layer. Accordingly, it may be appealing for nanoscale surface modification.

ACKNOWLEDGMENTS

We thank S. J. Chey, L. Huang, and M. M. R. Evans for stimulating discussions. This work was supported by the U.S. Army Research Office.

[1] M. P. Seah and D. Briggs, in *Practical Surface Analysis*, edited by D. Briggs and M. P. Seah (Wiley, New York, 1992), p. 1.
[2] S. Takeda, K. Koto, S. Iijima, and T. Ichihashi, Phys. Rev. Lett. **79**, 2994 (1997).
[3] D. Menzel and R. Gomer, J. Chem. Phys. **41**, 3311 (1964); P. Redhead, Can. J. Phys. **42**, 886 (1964).
[4] T. E. Madey and J. T. Yates, Jr., J. Vac. Sci. Technol. **8**, 525 (1971).
[5] For a recent review, see R. D. Ramsier and J. T. Yates, Jr., Surf. Sci. Rep. **12**, 243 (1991).
[6] K. Nakayama and J. H. Weaver, Phys. Rev. Lett. **82**, 980 (1999).
[7] R. J. Hamers, R. M. Tromp, and J. E. Demuth, Phys. Rev. B **34**, 5343 (1986).
[8] B. S. Swartzentruber, Y.-W. Mo, M. B. Webb, and M. G. Lagally, J. Vac. Sci. Technol. A **7**, 2901 (1989).
[9] B. Y. Han, C. Y. Cha, and J. H. Weaver, J. Vac. Sci. Technol. A **16**, 490 (1998); B. Y. Han and J. H. Weaver, Phys. Rev. B **58**, 10 981 (1998).
[10] B. Y. Han, C. Y. Cha, and J. H. Weaver, Phys. Rev. B **56**, 4966 (1997).
[11] X.-S. Wang, R. J. Pechman, and J. H. Weaver, Appl. Phys. Lett. **65**, 2818 (1994).
[12] R. J. Pechman, X.-S. Wang, and J. H. Weaver, Phys. Rev. B **51**, 10 929 (1995).
[13] Z. Zhang, M. A. Kulakov, and B. Bullemer, Surf. Sci. Lett. **369**, L131 (1996).
[14] T. Uda and K. Terakura, Phys. Rev. B **53**, 6999 (1996).
[15] Z. Zhang, F. Wu, H. J. W. Zandvliet, B. Poelsema, H. Metiu, and M. G. Lagally, Phys. Rev. Lett. **74**, 3644 (1995).
[16] J. van Wingerden, A. van Dam, M. J. Haye, P. M. L. O. Scholte, and F. Tuinstra, Phys. Rev. B **55**, 4723 (1997).
[17] B. Borovsky, M. Krueger, and E. Ganz, Phys. Rev. Lett. **78**, 4229 (1997).
[18] T. Yamasaki, T. Uda, and K. Terakura, Phys. Rev. Lett. **76**, 2949 (1996).
[19] R. J. Hamers, U. K. Kohler, and J. E. Demuth, J. Vac. Sci. Technol. A **8**, 195 (1990).
[20] Y. M. Mo, J. Kleiner, M. B. Webb, and M. G. Lagally, Phys. Rev. Lett. **66**, 1998 (1991).
[21] Z. Zhang, M. A. Kulakov, and B. Bullemer, Surf. Sci. **369**, 69 (1996).
[22] H. Feil, H. J. W. Zandvliet, M.-H. Tsai, J. D. Dow, and I. S. T. Tsong, Phys. Rev. Lett. **69**, 3076 (1992); H. J. W. Zandvliet, Surf. Sci. **377–379**, 1 (1997).
[23] B. C. Stipe, M. A. Rezaei, and W. Ho, Phys. Rev. Lett. **79**, 4397 (1997).
[24] Based on a one-dimensional heat transport model, each pulse at 35 mJ cm^{-2} produces a temperature rise of $\sim$250 K for $\sim$10 ns. Thermal desorption of GaAs is negligible at the peak temperature of $\sim$550 K.
[25] N. Itoh, J. Kanasaki, A. Okano, and Y. Nakai, Annu. Rev. Mater. Sci. **25**, 97 (1995); J. Kanasaki, A. Okano, K. Ishikawa, Y. Nakai, and N. Itoh, Phys. Rev. Lett. **70**, 2495 (1993); A. Okano, J. Kanasaki, Y. Nakai, and N. Itoh, J. Phys.: Condens. Matter **6**, 2697 (1994).
[26] A. Huijser and J. van Laar, Surf. Sci. **52**, 202 (1975); J. R. Chelikowsky and M. L. Cohen, Phys. Rev. B **20**, 4150 (1979).
[27] J. Kanasaki (private communication).
[28] J. Kanasaki, T. Ishida, K. Ishikawa, and K. Tanimura, Phys. Rev. Lett. **80**, 4080 (1998).
[29] M. Martel, Ph. Avouris, and I.-W. Lyo, Science **272**, 385 (1996).
[30] T.-C. Shen, C. Wang, G. C. Abeln, J. R. Tucker, J. W. Lyding, Ph. Avouris, and R. E. Walkup, Science **268**, 150 (1995). See also R. S. Becker, G. S. Higashi, Y. J. Chabal, and A. J. Becker, Phys. Rev. Lett. **65**, 1917 (1990); M. Schwartzkopff, P. Radojkovic, M. Enachescu, E. Hartmann, and F. Koch, J. Vac. Sci. Technol. B **14**, 1336 (1996).
[31] J. Xu, S. H. Overbury, and J. F. Wendelken, Phys. Rev. B **53**, R4245 (1996).
[32] H.-J. Ernst, F. Charra, and L. Douillard, Science **279**, 679 (1998).